

SEISMICITY AND 10-YEARS RECENT CRUSTAL DEFORMATION STUDIES AT ASWAN REGION, EGYPT

Mohamed S. ABDEL-MONEM, Haggag H. MOHAMED*,
Mohamed SALEH and Nadia ABOU-ALY

National Research Institute of Astronomy and Geophysics, Helwan

**Corresponding author's e-mail: haggaghm@yahoo.com*

(Received November 2011, accepted March 2012)

ABSTRACT

Since 1982, several study programs were initiated for monitoring seismicity, underground water behavior and recent crustal movements. The main characteristics of the seismic activity and the seismotectonics of the Aswan region are investigated based on the recently recorded seismic activity from 1982 to 2010 and the geodetic results. The results from these data sets are compared and combined in order to determine the main characteristics of deformation and hazard estimation in the Aswan region. GPS observations are being carried out by Aswan geodetic network twice a year since 1997 and still until now. Analysis of the repeated 10-years GPS campaigns from the network revealed horizontal movements at the level of 7–10 mm/a. The estimated strain rate tensors show compression and tension components in the directions WNW-ESE and NNE-SSW which consistent with the P- and T-axes derived from earthquake fault plane solutions, respectively. The network area has been suffered from post-seismic deformation during the present interval; hence an increase in the general earthquake activity in the area could be expected.

KEYWORDS: seismicity; GPS network; recent crustal deformation; Aswan region

INTRODUCTION

Aswan region is located within the stable platform of Northern Africa. The Nile follows the contact between surface exposure of the granite of the Eastern Desert to the East, and the sedimentary cover of the Nubian sandstone to the West. The Nubian plain covers most of the area southwest of Aswan City and borders of the reservoir from the West (Issawi, 1969, 1978). The Nubian plain is relatively flat, and the surface has an average elevation of 200 m above the mean sea-level. The structural pattern of the Aswan region is governed mainly by faulting. Faults that dissected the area (Fig. 1) were classified according to their trends into E-W and N-S faults. The E-W fault system includes Kalabsha fault that crosses along Gabel Marawa, it was identified as the most active fault in the area and the source of 1981 earthquake (Kebeasy et al., 1987) and the Seiyal fault which is approximately 12 km to the north of Kalabsha fault. While the N-S fault system is represented by several fault segments, which run nearly parallel to the main course of Lake Aswan shore (Fig. 1). It includes Gabel El-Barqa fault, Kurkur fault, Hour El-Ramla fault, Gazelle fault and Abu Dirwa fault. The intersection of the N-S and E-W faults is characterized by high seismicity on the Kalabsha fault zone.

Occurrence of the November 14, 1981 earthquake in Kalabsha area encouraged seismo-

logical studies to be carried out in Aswan area (e.g. Kebseay et al., 1982; Raafat and Haggag, 2004; Haggag et al., 2008). Aswan seismicity is concentrated on the Kalabsha fault zone, which trends E-W over a distance 300 km (Issawi, 1982), particularly along its most eastern segment. The most eastern part of the Kalabsha fault is located beneath the lake (Wadi Kalabsha embayment) and has been suffered by the November, 1981 earthquake. The water extension in the Kalabsha embayment varies simultaneously with the water level changes in the main part of Lake Aswan. The water level in the lake varies daily and fluctuates four times during the year according to the cycles of inflow and discharge.

INDUCED SEISMICITY

One of the more interesting aspects of the induced seismicity at Aswan region is the possible role that the Nubian sandstone plays in the control of the small size earthquakes activity. The sandstone surrounding the reservoir area is highly porous (25 %) and relatively permeable compared to the underlying granite. As the reservoir fills, the expanding area of the reservoir and the rising water level allow water to seep into the sandstone, thus the local water table raises. Because of the impermeable basement, the water is confined to the westward thickening sandstone lens.

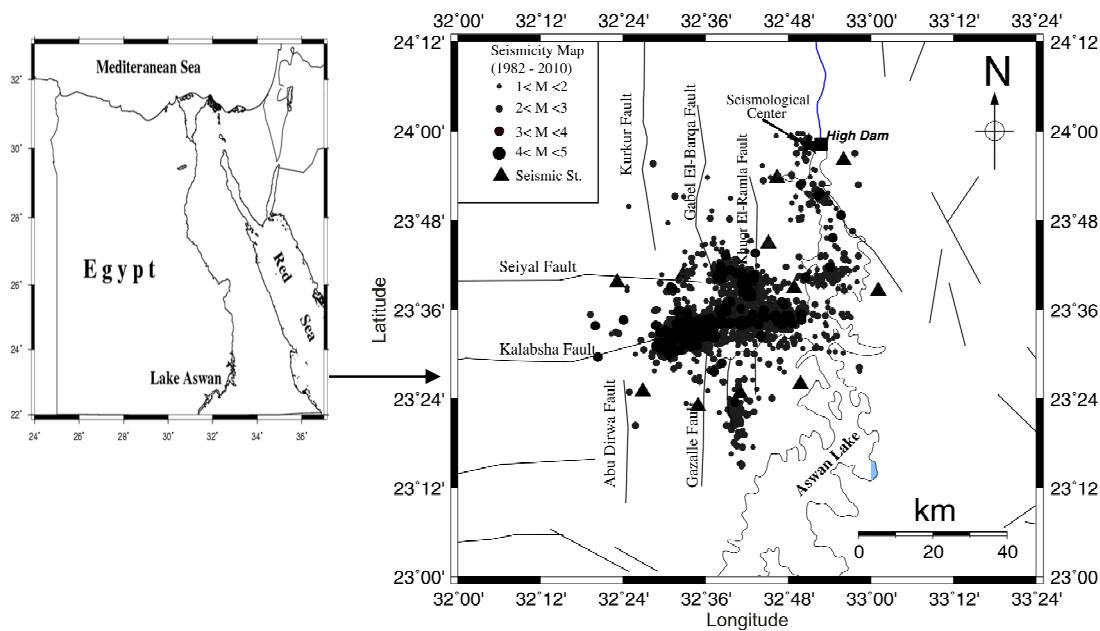


Fig. 1 Micro-earthquakes recorded by Aswan Seismic Network from 1982 to 2010.

The seismicity is concentrated on the Kalabsha fault zone, particularly, along its most eastern segment, which is located beneath a large area covered by water (Fig. 1). However, the E-W Kalabsha fault system controls the seismicity in the Lake Aswan area. About 95% of the seismic activity is located in the area enclosed by Latitudes 23.400 N - 23.800 N and Longitudes 32.400 E - 33.000 E, under a major western branch of the lake, at the intersection between the E-W and N-S fault trends. A few epicenters were located in the mainstream of the Nile between the High Dam and Wadi Kalabsha. There are seismic activities occurring along the other fault trends (e.g., Seiyal, Khour El-Ramla and Gazalle). Kalabsha fault is a right-lateral strike-slip fault and consists of several segments forming a conjugate fault pattern (Issawi, 1982). The seismicity is separated into shallow and deep seismic zones. Shallow earthquakes have focal depths less than 12 km while the deep events extend from 12 to 28 km as shown in figure 2. The deeper activity is taking place where the intersection of the easterly trending Kalabsha fault with the northerly trending faults beneath Gebel Marawa. The activity outside Marawa area is shallower, i.e. 0-12 km. Deep events are related to their magnitude. Events of magnitude ≤ 1 occur at depth less than 10 km (Fig. 2a), where depth of the earthquakes are increasing with increasing their magnitudes.

Hassoup et al., 2005 suggested that at shallow depth, conditions with more heterogeneous material properties and lower lithospheric stress prevail. The reverse conditions prevail at greater depth (11-30 km).

So, the shallow events may be classified as seismicity induced by the water reservoir and that the earthquakes in the Lake Aswan area occur due to its tectonics and the presence of the water lake.

In Figure 3 the number of earthquakes is presented in terms of one year for the time period 1882 to 2010, where M is the magnitude. The level of seismicity is decreasing with time although the water level (amount) in Lake Aswan fluctuated during the same period but the activity has begun to increase again in the last three years specially earthquakes with $M \leq 2$.

SEISMICITY AND THE WATER LEVEL VARIATION IN THE ASWAN LAKE

Reservoir induced seismicity have been reported from many parts of the world (Gupta, 1992; Talwani, 1997). The direct correlation of the pronounced increases in seismicity with the first filling of the reservoir is observed in some reservoirs. However, there are cases in the reservoirs were directly responsible for the increased seismicity (Gupta, 1972; Simpson, 1976; Gupta and Rastogi, 1976, Kebsay et al., 1982). Simpson et al., 1988 identified Aswan seismicity as being reservoir-triggered sequence particularly after the occurrence of a remarkable seismic sequence in August 1982 during the period of seasonal increase in the lake water level. Since 1982, earthquakes of small-magnitude ($M < 5$) have characterized Lake Aswan area.

Correlation between the seismicity and the water level variations in Lake Aswan provides great

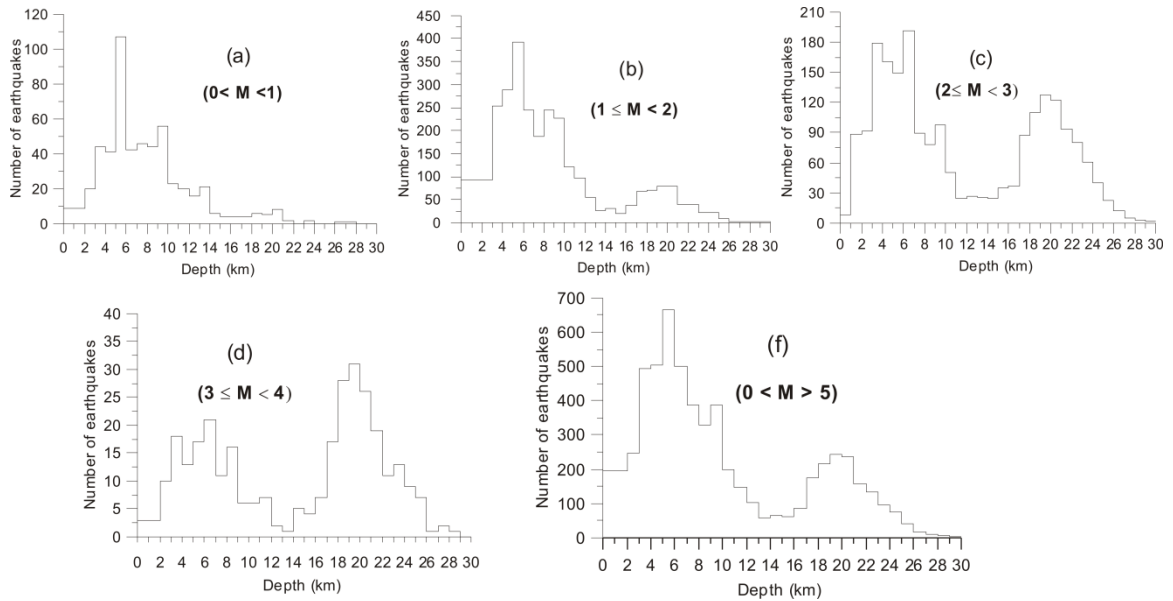


Fig. 2 Frequency of earthquake focal depths at Aswan region (of different magnitudes) during the period 1982-2010.

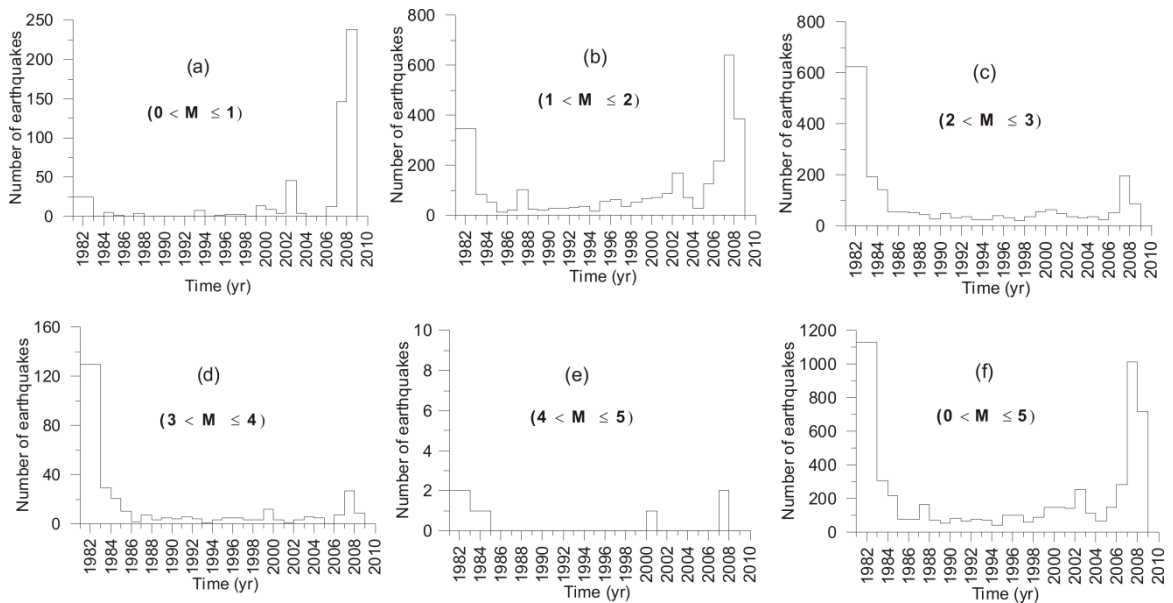


Fig. 3 Frequency of earthquakes (of different magnitudes) with time at Aswan region during the period 1982-2010.

suggestion to distinguish the earthquakes, particularly those in shallow seismic zone in the reservoir-triggered seismicity category. The correlation between temporal variations in seismicity and water-level changes in the lake are presented in terms of one year interval changes in the lake level and earthquakes of magnitude ≥ 0.1 for the time period from 1982 to 2010 (Fig. 4). The figure shows clearly a gradual decrease of the average seismicity is clear with the exception of some spikes in micro-earthquakes. Concentration of the seismic activities (swarms)

appears in specific periods (i.e., during August 1982, June 1987 and April 2007), more detailed information about these swarms is possible to obtain from Haggag and Karrar (2009).

The figure indicates also that, the direct correlation between these variables and inducing the earthquakes is not obvious with all the event sequence; it may be related to the delay time for inducing the seismicity. The time required for inducing the earthquakes is unknown until now. Slowly of the water diffusion from the surface into the

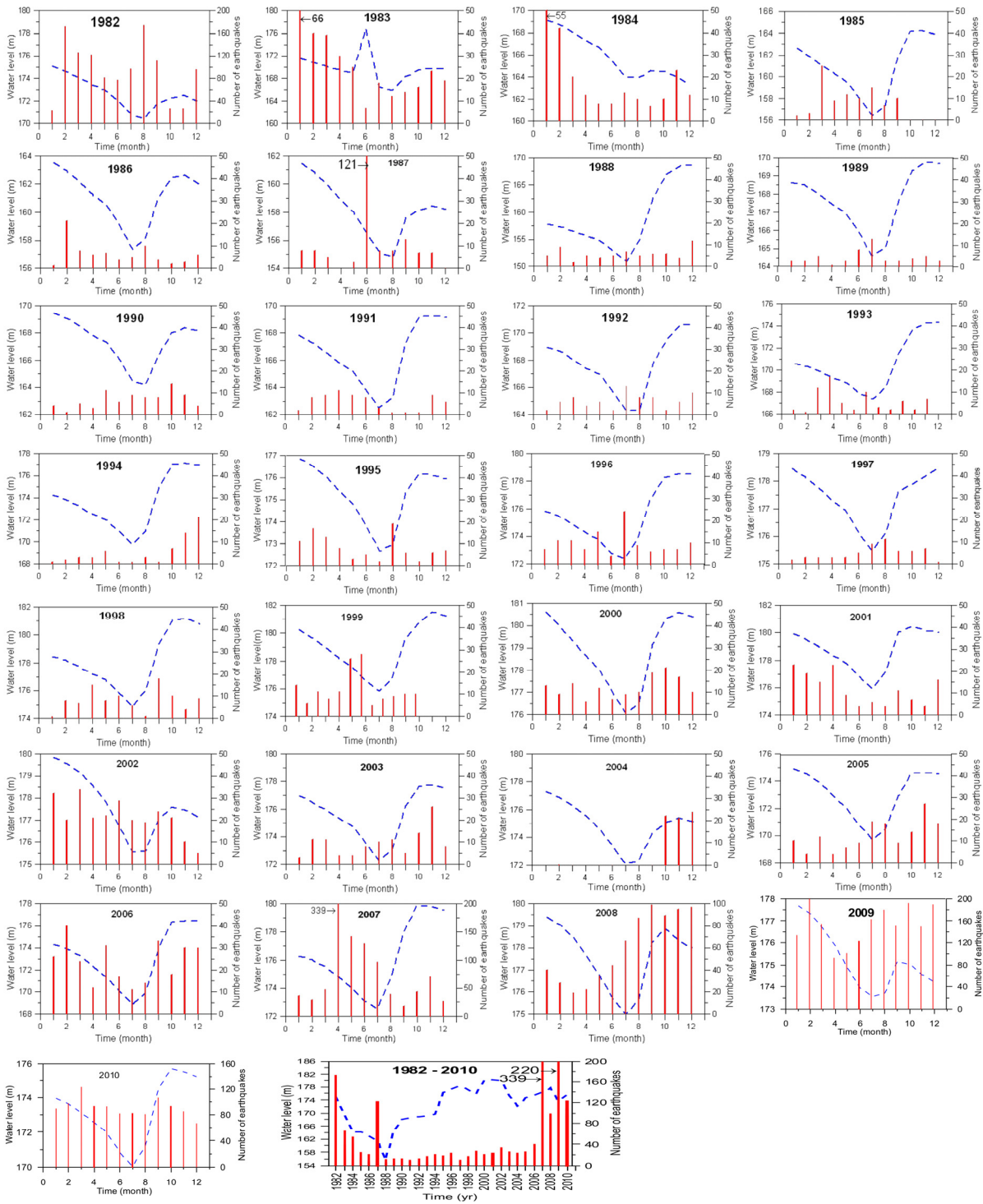


Fig. 4 Water level in the lake and number of the earthquakes occurred within the considered area for the period 1982 to 2010.

sandstone may explain the delay time between the filling of the reservoir and the start of the seismic activity. The time required for triggering micro-earthquakes depends on a several factors, e.g. kind of faults, thickness of the sandstone layers and their porosity, amount of water stores in the sandstone, the presence of specific geological conditions and the local tectonic setting. All these phenomena may have

an active role in the delay time for several days or months for triggering micro-earthquakes. Therefore, the Nubian Sandstone plays a quite suitable medium controls the activity of micro-earthquakes.

The water factor in the reservoir performs as an activating medium in triggering the micro-earthquakes. Increasing the reservoir load is not only because of the water within the reservoir, but also due

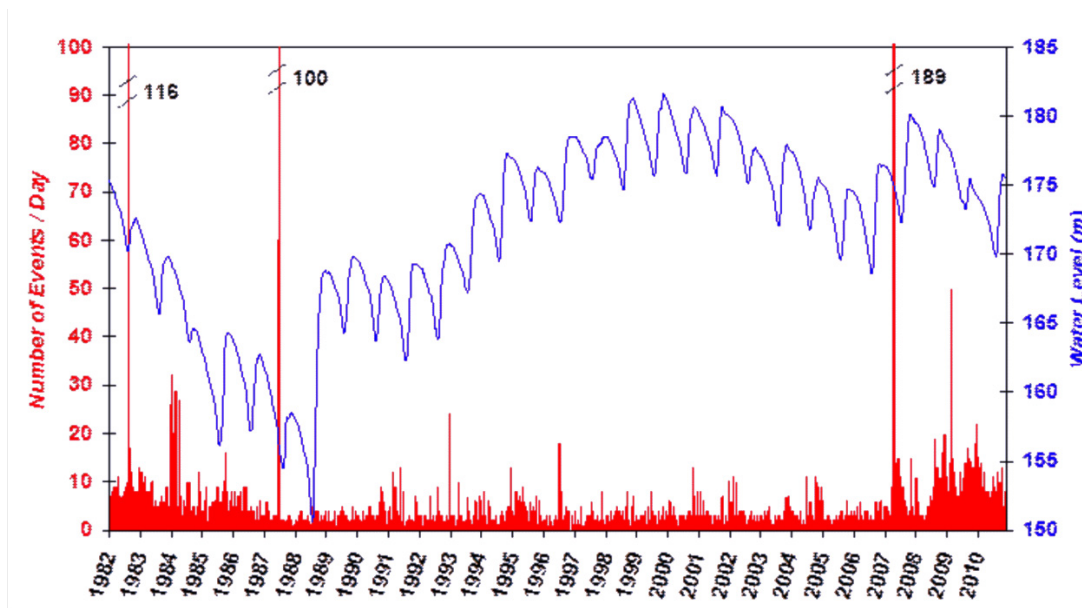


Fig. 5 Relation between Lake Aswan water level and seismicity during the period 1982- 2010.

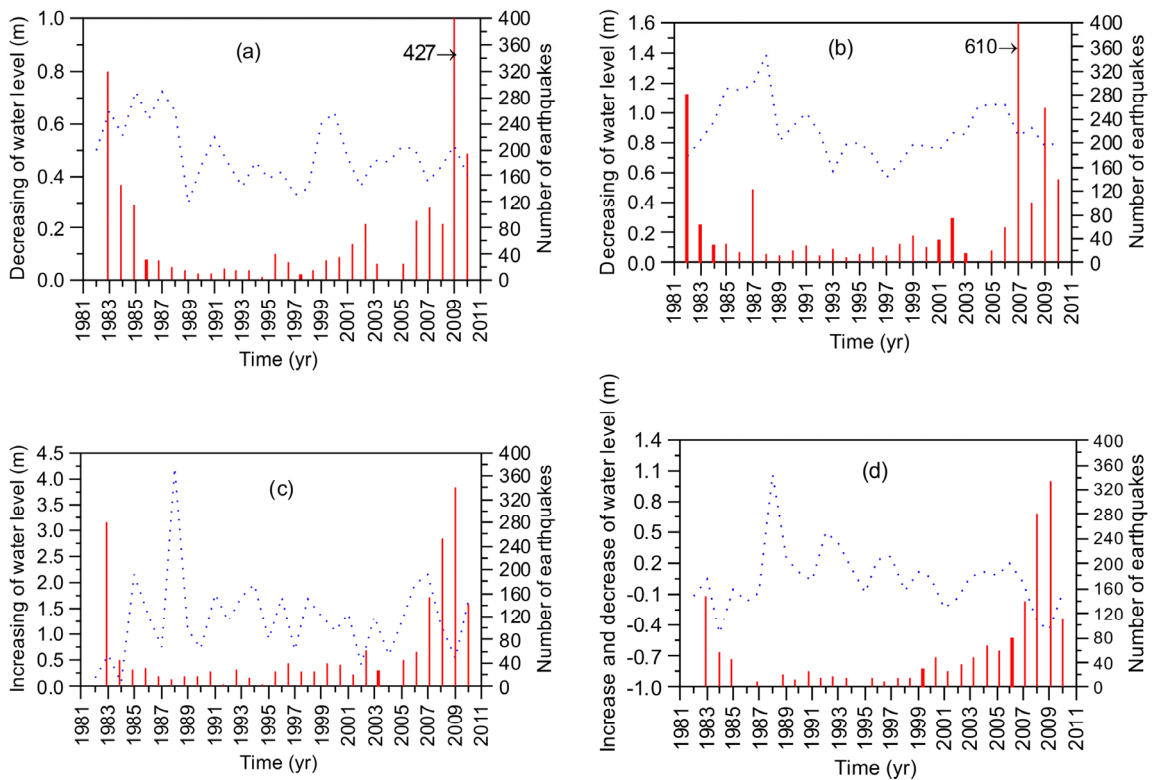


Fig. 6 Relation between the average increasing and decreasing of water level (dashed line) and totals of earthquake frequency ($M_L > 0.1$ to 5) (vertical bar) for the same months at Lake Aswan. (3 months/year) from 1982- 2010. (a) January, February, and March. (b) April, May, and June, (c) July, August, and September (d) October, November and December.

to a significant amount of water that stored in the sandstone (Kebeasy and Gharib, 1991; Abdel-Monem, 1994). The increased pressure at the base of the sandstone results from the combined influence of both the water in the reservoir and the increased water table in the sandstone. The time required for the water to diffuse into the sandstone may explain the delay between the filling of the reservoir and the starting of the seismic activity in the area. Lateral and vertical variations in permeability, caused by faults and aqueducts, may be important in determining the distribution of water within the sandstone and the access of pore pressure to faults. It is essential to monitor the current distribution of the water table and its changes with time to determine how quickly it will reach equilibrium. Figure 5 shows the daily water level changes in the lake and number of earthquakes that occurred in the area during the period from 1982 to 2010. It is also characterized by an annual cycle of the water level variation with peak and trough being often observed yearly during November-December and July-August, respectively. The figure shows clearly a gradual decrease in the average seismicity with the exception of some spikes in micro earthquakes. Concentration of the activities appears in specific periods (i.e., during August 1982, June 1987, April 2007). It is also observed that the direct correlation between these variables is not clear.

Figure 6 illustrates the relation between the average changes of the water level and totals of earthquake frequency. Data for 26 rainy seasons from 1982 to 2010 provides 26 such examples, where the rainy season extends yearly from July to October. It is clear that there is no obvious increasing in the seismic activity level related to the increasing or decreasing in the water level over this time period. A careful examination of this figure shows that every year, following the rainy season, the activity slightly increases (Fig. 6a) while the relation is not clear as shown in Figure 6 (b, c, d), then the activity increased during the last four years 2006, 2007, 2008 and 2009.

B-VALUE SCANNING

The seismic b-value is defined by Gutenberg-Richter (1954) as the relationship between magnitude and event occurrence, it is a measure of the proportion of larger to smaller events within a set of earthquakes. Temporal scanning of the b-value in the frequency-magnitude relationship could be used as an indicator for the stress condition in the seismically active regions. The frequency distribution of earthquakes over an observed range of magnitudes in a particular area can be represented by the formula:

$$\text{Log } N = a - bM \quad (1)$$

where N is the cumulative number of earthquakes of magnitude greater than or equal to M and a and b are constants.

The constant a depends on the sample size and it is found to vary from region to region (Gupta and Rastogi, 1976) whereas the parameter b commonly called the b-value, it is a measure of the relative number of large and small events in the sample. This relation is considered as important criteria for comparing the seismicity of different studied areas. It can be hold for all magnitude ranges, in all locations and all times Runddle (1989). Mogi (1962b) and Scholz (1968) indicated that a very fundamental physical property of the fracture process would be discovered if the Gutenberg-Richter relation could be explained completely and the physical meaning is understood.

Abdel-Monem (2005) had presented and analyzed seismic data recorded by Aswan Seismic Network, the b-values for Aswan region was estimated. For the proposed study the area, a linear regression analysis was carried out to estimate the coefficients of the Gutenberg-Richter relation between the magnitude and their $\log N$ (Fig. 7). The frequency-magnitude relationship for the data ranging from magnitude 2.3 to 3.8 is found to give the best fit in the linear relation as:

$$\text{Log } N = (5.097 \pm 0.044) - (1.065 \pm 0.017) M \quad (2)$$

And per year it is:

$$\text{Log } N = (4.37 \pm 0.044) - (1.065 \pm 0.017) M \quad (3)$$

SEISMIC HAZARD ESTIMATION

The term seismic hazard is used here to denote the probability of occurrence of an earthquake with magnitude larger or equal to a particular value within a specified region and a given time span (Epstein and

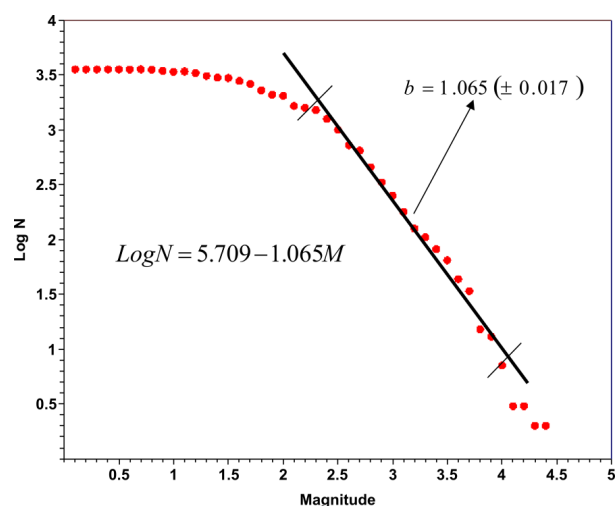


Fig. 7 A cumulative frequency of earthquakes as a function of magnitude for Aswan region. Only data between 2.3 and 3.8 were used to derive the least squares fit to the data.

Table 1 Seismic hazard for Aswan region (values represent the probability of an earthquake of a particular magnitude in the specified time period).

Magnitude	Time (yr)						
	1 (%)	5 (%)	10 (%)	20 (%)	50 (%)	100 (%)	200 (%)
3	98	0.99	100	100	100	100	100
4	31	84	97	99	999	100	100
5	3	14	27	47	80	96	998
6	0.2	1	2	5	13	24	42
7	0.02	0.1	0.2	0.5	1	2	4

Lomnitz, 1966; Howell, 1980; Edel, 1984). The Gumbel distribution was applied for calculating the probability of occurrence of an earthquake at Aswan region.

$$G(m) = \exp(-\alpha \exp(-\beta m)) \tag{4}$$

where m is some earthquake magnitude such as ($M < m$), and " α " and " β " are calculated as follows:

$$\alpha = \exp(a \ln 10) \text{ and } \beta = b \ln 10 \tag{5}$$

Epstein and Lomnitz (1966) further showed that the model (most probable or most frequently observed) annual maximum magnitude \bar{m} is:

$$\bar{m} = (\ln \alpha) / \beta \tag{6}$$

The model maximum magnitude \bar{m}_T in some T year time period is:

$$\bar{m}_T = \bar{m} + (\ln T) / \beta \tag{7}$$

They also demonstrated that the earthquake hazard ($R_T(m)$), i.e., the probability of occurrence of an earthquake of magnitude m or greater in a T year period, can be found using:

$$R_T(m) = 1 - \exp(-\alpha T \exp(-\beta m)) \tag{8}$$

The Gumbel distribution is useful for comparing present and past seismicity because it is concerned with the largest earthquakes in the record. As a check on the Gumbel distribution, the model annual maximum magnitude \bar{m} was calculated from equation (6) using the recent earthquake data set. A second check made by computing the expected maximum magnitude \bar{m}_T for period of the data set using the equation (7). The regional hazard or probability of an

earthquake in a particular time period was calculated from equation (8).

The term seismic hazard is used here to denote the probability of occurrence of an earthquake with magnitude larger or equal to a particular value, within a specified region and a given time span. The occurrence of large size earthquake in the next 200 years is estimated to be with magnitude 5 as shown as in Table 1 and Figure 8.

GPS MEASUREMENTS AND DATA ANALYSIS

The used data were collected from Aswan geodetic network, during the period from 2001 to 2010, which consists of 11 stations and covers the northern part of Lake Aswan. There are 7 stations along the western side of Lake Aswan and 4 stations along the eastern side (Fig. 9). The campaign observations are repeated twice a year since 1997. The GPS observations are carried out using Trimble receivers 4000 SSI under constant conditions, such as: the satellite-masking angle is 15 degrees, the sampling

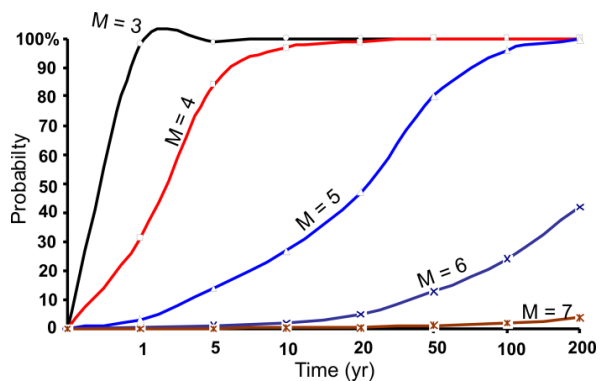


Fig. 8 Probability of an earthquake of a particular magnitude in specified time period is a plot for Aswan region.

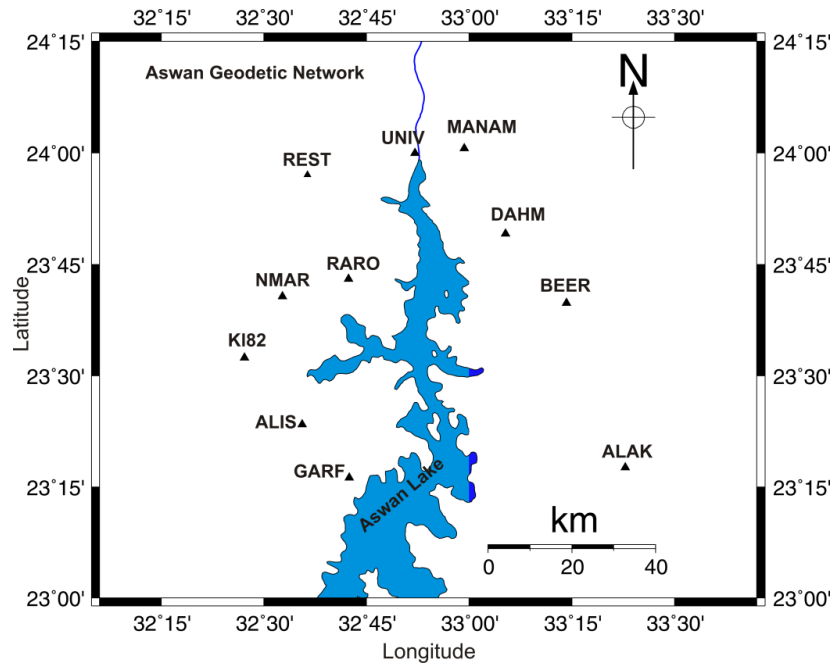


Fig. 9 Configuration of Aswan geodetic network.

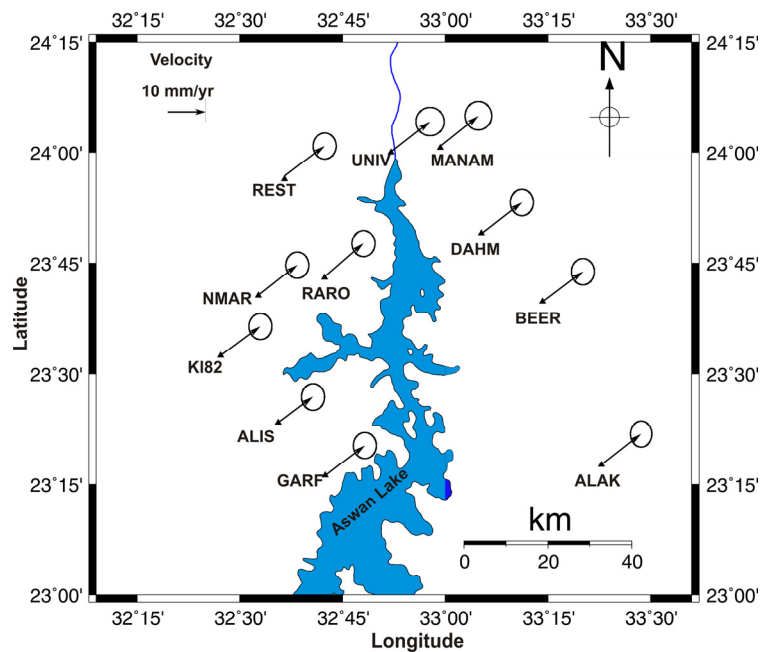


Fig. 10 The horizontal velocity of Aswan geodetic network (including the velocity of the African plate).

interval is 30 seconds and the observation time in all sessions is 72 hours at all stations. The used GPS data in this study were processed using Bernese V. 5.0 software program (Dach et al., 2007).

Another software program for adjustment and deformation parameter calculations was used (Fuji,

1997). International GPS Service (IGS) permanent stations Ankara “Ankr” in Turkey, Not1 “Not1” in Sicilia, Dragot “Drag” in Israel and Bahrain “BAHR” in Bahrain were applied in the processing of the GPS data. The network is tied to (IGS) stations in order to compute the precise coordinates of all stations of the

Table 2 The geodetic stations and annual horizontal velocity at Aswan region including the velocity of the African plate.

STATION	Longitude	Latitude	VE (mm)	VN (mm)	δE (mm)	δN (mm)
ALAK	33.38034741	23.29424896	26.7	21	2.4	3.0
BEER	33.2370786	23.66440271	23.4	17.2	2.6	3.0
DAHM	33.08807935	23.8187234	26.6	20.2	2.6	3.0
MNAM	32.98837098	24.01513563	25.5	20.4	3	3.2
UNIV	32.86852325	24.00196377	26.1	20.4	3.2	3.2
REST	32.60934967	23.94755829	26.8	20.1	2.6	3.0
RARO	32.7060345	23.71886076	26.2	22.9	2.6	3.0
NMAR	32.54454204	23.67803407	26.3	20.3	2.6	3.0
KL82	32.45286874	23.54096545	27.1	20	2.6	3.0
ALIS	32.59331359	23.39064669	27.2	20.7	2.6	3.0
GRAF	32.70790448	23.27056083	26.8	19.9	2.6	3.0

Table 3 The geodetic stations and annual horizontal velocity at Aswan region including the velocity of the African plate.

STATION	Longitude	Latitude	VE (mm)	VN (mm)	δE (mm)	δN (mm)
ALAK	33.38034741	23.29424896	6.56	4.32	1.312	0.864
BEER	33.2370786	23.66440271	4.42	10.48	0.884	2.096
DAHM	33.08807935	23.8187234	5.94	7.24	1.188	1.448
MNAM	32.98837098	24.01513563	7.88	4.98	1.576	0.996
UNIV	32.86852325	24.00196377	3.36	6.70	0.672	1.34
REST	32.60934967	23.94755829	6.92	9.32	0.692	0.932
RARO	32.7060345	23.71886076	6.92	9.32	1.384	1.864
NMAR	32.54454204	23.67803407	8.04	5.84	1.608	1.168
KL82	32.45286874	23.54096545	10.50	6.56	2.1	1.312
ALIS	32.59331359	23.39064669	17.52	16.06	3.504	3.212
GRAF	32.70790448	23.27056083	5.56	9.34	1.112	1.868

network in International Terrestrial Reference Frame (ITRF 2005).

The displacement vectors at each GPS station were determined under an assumption of free network adjustment. The obtained values were adjusted to get more accurate positions of the GPS stations. Horizontal components at each station were computed from the difference of adjusted coordinates of the stations from one epoch to another and from the last epoch to the first one. In this study, we have used the final analyses between the last epochs to the first one. The horizontal components of displacement vectors with 95% confidence error ellipses are shown in Figure 10. The error ellipses represent standard error

in all direction around the observed site. The horizontal displacement vectors are of magnitude ranging of 15-25 $5 \text{ mm} \pm 3.1 \text{ mm/yr}$. Figure 10 and Table 2, show the annual horizontal velocity of this region including the annual horizontal velocity of the African plate.

Bernese V 5.0 (Dach et al., 2007) used to compute the common sets of the coordinates and velocities for epochs from 2001 to 2010. Horizontal velocities, given in Table 2 and Figure 10 show the sum of regional and local velocity. The figure shows also the dominant movement of the African plate. In order to reveal the local horizontal velocity at Aswan region, the effect of African plate movement has to be

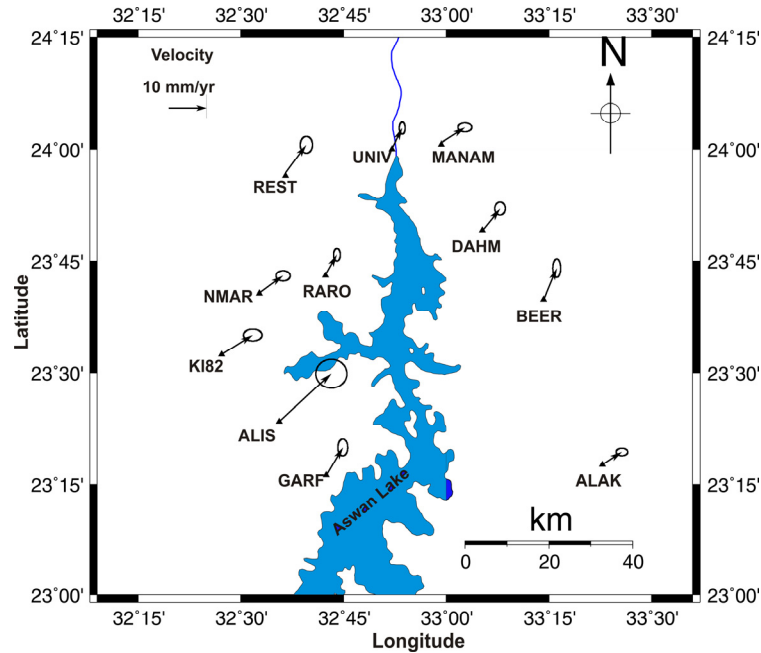


Fig. 11 The residual annual horizontal velocity of Aswan geodetic network.

removed. So, the annual horizontal velocity at Aswan region can be obtained by extracting the values of the African plate, deduced from model Nuvell 1A (McClusky et al., 2003) from the observed velocity as shown in Figure 11 and Table 3.

In Figure 11, stations located on the eastern side of the Lake Nasser move in the direction of northeast with an average rate of $4\text{mm} \pm 1.1\text{mm}$ per year, while those on the western side of the Lake Nasser move in the direction of north to northeast with an average rate of $6.5\text{mm} \pm 1.15\text{mm}$ per year.

ESTIMATION OF THE DEFORMATION PARAMETERS

In numerous applications of deformation analyses in crustal deformation studies, the final aim is the representation of the deformation in terms of strain parameters. The basic principles of strain analysis, as developed in the theory of elasticity, are applicable, if the area covered by the monitoring network can be considered as a continuum deforming under stress. The areal compression strains cover the medial area towards the south in the present period, where the intersections of the N-S faults with the Kalabsha fault. Dilatational strains show patches of high and medial values of the compression strain (Fig. 12). In addition to this, there are low compressions in the eastern and the northern parts of the area as well as in its eastern part.

The total amount of maximum shear strain accumulation during the present interval is relatively small and lies in the lowest class (according to Fuji's classifications, 1995) and is prevailing in the central part of the area, where there is an intersection

of N-S fault with Kalabsha fault (Fig. 13). The network area can be divided into three parts: high shear strain part covers a part of the Kalabsha, Seiyal and Khor El-Ramla faults. Medial shear strain part covers some parts in the area while, the low shear strain rate covers most parts of the area. To compare the maximum shear strains with the seismic data; the epicentral distributions are plotted (Fig. 13). Generally, high rates of the maximum shear and horizontal strains with earthquake activity of the present interval in the central part indicate that the rocks of that area are characterized by a property of plasticity, so, when any deformation happens it could be the capability to return back again to the normal case. This might be due to the restraining and releasing of stress along the active faults in the area, Kalabsha, Seiyal and Khor El-Ramla faults.

The present analysis shows that, the medial part of the area in the present period is dominated by compressional strain, shear strain and horizontal strain rates. This might be due to the restraining and releasing of stresses in that area. From this analysis, the hazards could be evaluated in the Kalabsha, Seiyal and Khor El-Ramla parts. The crustal deformation processes could occur during the accumulation of the energy within the Earth's crust and during the different paths of energy releasing. This means that, the network area has been suffered from post-seismic deformation during the present interval. However, a dramatic increase in the general earthquake activity in that area could be expected. The seismic activity reflects the release of energy accumulated as a result of the pressures accumulated in the area.

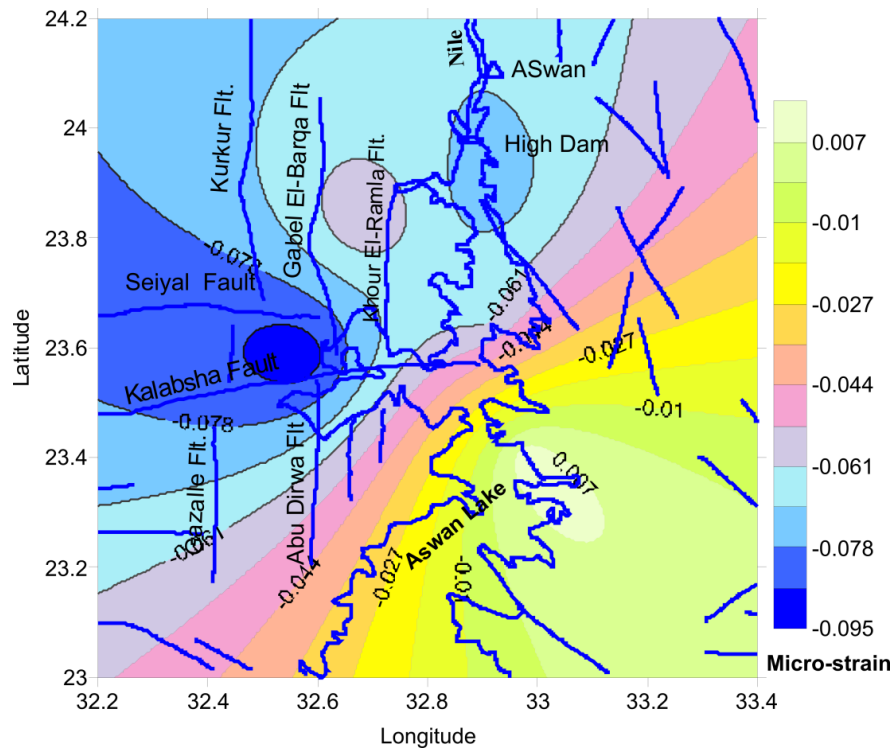


Fig. 12 Distribution of the dilatation strain rates at Aswan region.

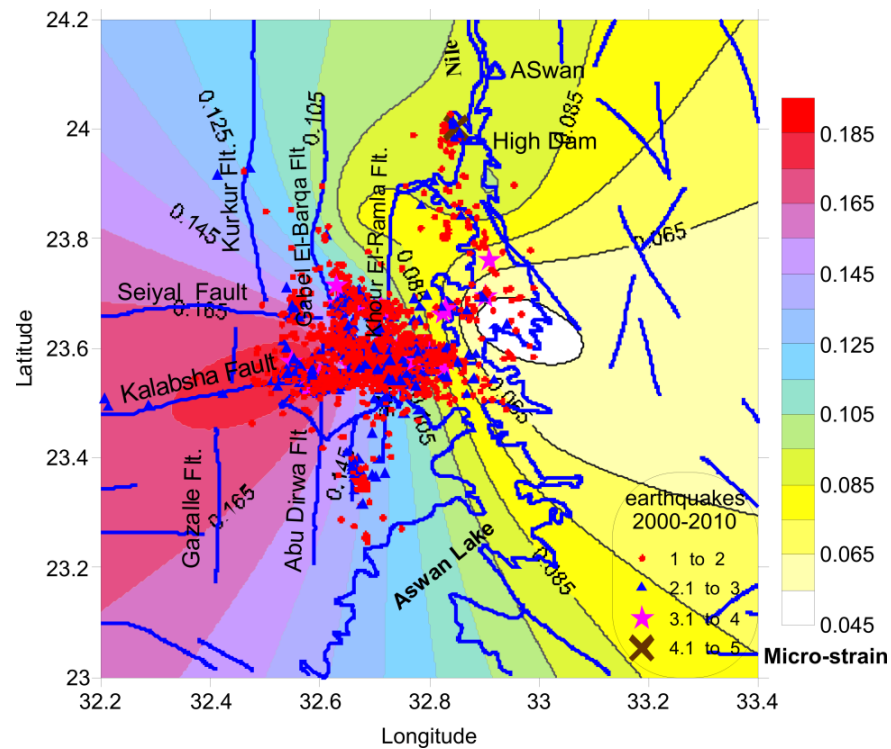


Fig. 13 Distribution of the maximum shear strain rates at Aswan region.

Table 4 Deformed stations (mm) calculated in three dimensions during the period 2001- 2010.

Year		2001	2002	2003	2004	2005	2006	2007	2008	2009	2010
Station											
RARO	N	3.41	0.07	6.14	1.04	-0.1	-2.55	-0.51	-4.04	-4.22	3.48
	E	4.22	-2.57	0.03	0.93	0.42	-0.25	-2.32	0.63	-1.22	0.48
	U	-0.69	-1.17	13.74	-14.49	-11.99	-9.13	19.55	-6.8	7.39	-4.25
NMAR	N	-2.55	1.25	-1.75	0.72	0.87	1.13	-5.63	5.55	0.2	-0.8
	E	-2.01	-4.35	-1.04	-1.11	-1.21	-1.53	6.66	-1.11	-2.54	8.02
	U	5.32	-4.23	12.65	-9.39	-16.4	-14	0.34	-1.54	18.27	3.31
KL82	N	5.82	-1.96	-1.79	2.17	1.81	0.26	-7.36	-0.81	9.5	-7.27
	E	-2.39	2.78	-1.0	-0.25	-2.32	1.67	2.89	-1.61	2.34	-2.18
	U	11.12	2.91	15.63	-14.48	-14.81	-9.56	-26.9	-11.32	32	-4.04
ALIS	N	2.27	-0.26	1.51	-0.49	-	-0.22	-1.83	6.44	-7.23	0.46
	E	-5.84	2.38	1.01	-1.48	-	-1.38	-0.7	4.43	0.15	2.39
	U	-15.8	-4.79	5.28	0.4	-	-7.02	2.5	-2.56	54.85	-3.9
GARF	N	-4.51	-3.88	-1.7	-3.08	-0.72	-0.92	1.37	3.35	2.89	5.13
	E	9.42	-8.83	0.58	-2.46	-1.45	2.26	-4.03	-0.72	7.04	-1.11
	U	4.78	21.6	3.44	4.01	19.4	10.22	-31.35	17.92	-109.67	18.78
ALAK	N	-1.81	-1.67	0.15	-0.43	3.01	1.45	0.02	-4.03	-	1.89
	E	-4.62	-2.51	-1.66	-4.11	3.29	0.74	3.37	3.82	-	-1.22
	U	-15.89	-23.03	11.81	7.64	-0.32	31.46	-6.77	32.61	-	-11.76
BEER	N	12.18	2.76	8.53	9.96	-8.71	-4.61	-6.63	-3.8	-	-5.68
	E	6.73	3.36	5.94	13.3	-11.63	-9.26	-0.36	-9.64	-	5.55
	U	-9.68	-9.62	-2.51	-8.47	-3.75	66.18	-5.31	-0.71	-	-6.48
DAHM	N	3.86	-0.92	-1.67	-2.29	4.0	5.29	-3.99	3.57	-	-8.84
	E	-1.64	-0.44	-2.23	-1.02	0.1	1.37	6.7	-0.96	-	-2.3
	U	17.58	19.79	-0.22	1.52	12.08	-109.2	12.65	6.92	-	12.44
MNAM	N	-2.44	-0.35	0.12	-1.24	-5.4	1.97	0.04	3.66	1.16	-0.53
	E	-1.76	1.69	-1.37	-0.45	-5.7	5.29	6.52	-2.81	1.34	-4.34
	U	7.14	19.27	33.74	-9.64	1.51	-4.41	-93.89	3.56	-12.16	13.24
UNIV	N	-4.39	-1.52	-1.73	-3.75	-2.11	4.35	1.92	0.47	0.26	5.91
	E	-0.4	1.86	-0.25	1.62	1.4	1.04	-1.04	-3.87	-0.24	0.08
	U	-4.98	2.12	12.82	-21.93	-23.69	-15.58	72.84	-7.05	-24.27	0.97
REST	N	2.37	-7.57	-0.96	-2.39	-1.37	-0.68	8.08	-4.06	1.73	6.25
	E	-1.26	6.62	1.64	1.19	2.08	0.46	-1.52	-4.68	-0.12	-5.42
	U	-6.89	-30.05	-84.44	56.44	52.32	31.96	70.95	7.21	-5.22	-18.36

TIME SERIES ESTIMATION

Geodetic Time Series is a temporal variation of the estimated geodetic and geophysical parameters. A lot of information can be extracted from the geodetic time series; it can give us the stability of each station. The annual velocity of each station and its direction, seismic cycles, expected time for the activity along the faults and extract the seasonal effects of the GPS observations, improving the models for ocean loading and tropospheric corrections are used in the computations of the strain parameters.

Here a geodetic time series was made for Aswan network from the processing of the GPS data of the ten campaigns (10 years). Processing the above GPS

data yielded the precise coordinates of all stations. Table 4 shows the deformed stations while Figure 14 shows the time series graphs in north and east directions. In this figure, each small solid circle on the plot represents an independent position estimate typically, based on three days of observations (one campaign), with error bars. The blue lines represent the linear horizontal velocity, while the dots represent the individual solution for each campaign. For the deformation analysis results, it can be notice that most of the deformed stations in all epochs are large in the North direction than in the East direction except BEER station where there is an error in its concrete. The magnitudes of the deformed stations are variable

from one epoch to another and inhomogeneous over the area. The orientations of the pressure and tension stresses in the Aswan region are ESE-WNW and NNE-SSW, respectively.

DISCUSSION AND CONCLUSIONS

Seismicity and the crustal deformation in the seismically active areas in Aswan area were examined as obtained from both the seismic and GPS data. The results from these data sets are compared and combined in order to determine the main characteristics of deformation and hazard estimation in the Aswan region. Comparing the geodetic results with the seismic activity in the area elucidated a relationship between the accumulated energy releases associated with the earthquake occurrences and the deformation. This relationship has been interpreted as the seismic activity being reflects the release of energy accumulated as a result of the stress accumulated in the region. The strain rate tensors estimated in this study show compression and tension components directed in the WNW-ESE and NNE-SSW directions that are consistent with the P-axes and T-axes derived from earthquake fault plane solutions, respectively. The compiled output from the seismological and geodetic analysis threw lights upon the geodynamical regime of these seismo-active areas and put Aswan region under the lowest class according to horizontal crustal strains classifications.

Study of the inducing seismicity from the water level variation in Lake Aswan is of great importance and play great roles necessity for the safety of the High Dam body. So, this study achieved a better understanding of the seismicity and recent crustal deformation at Aswan region by a suitable treatment based on available earthquake recording data. This study is an attempt to build a basis for further development of seismic catastrophic risk management models to reduce a risk of large catastrophic losses within the important region in Egypt. The conclusion of the present investigation can be summarized as follows:

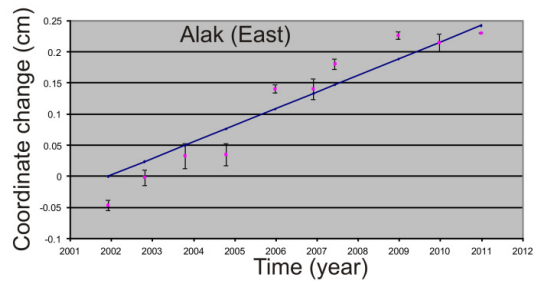
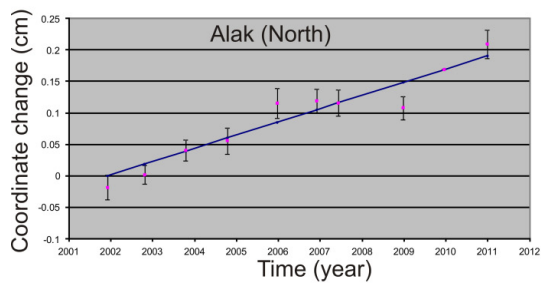
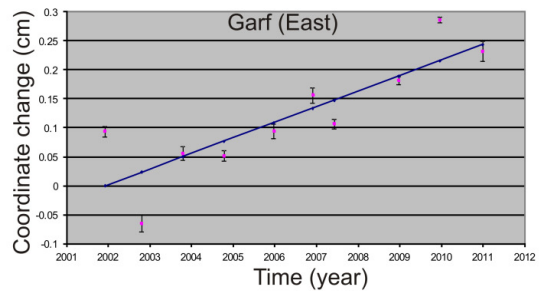
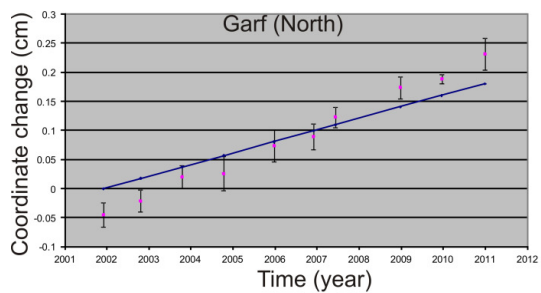
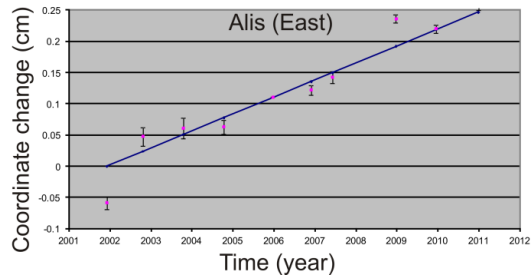
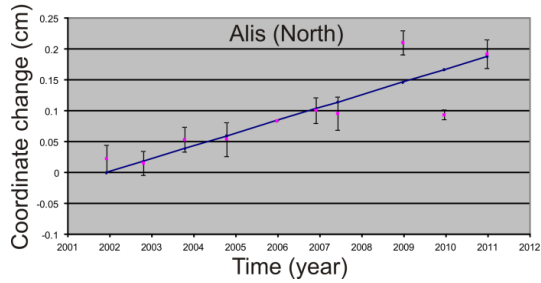
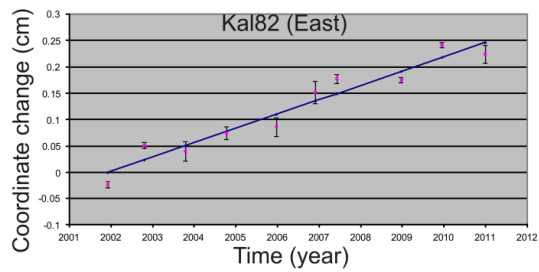
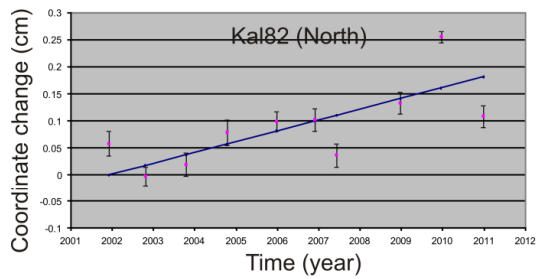
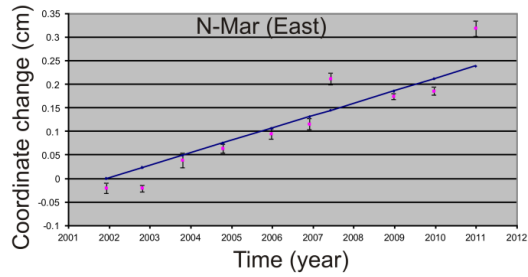
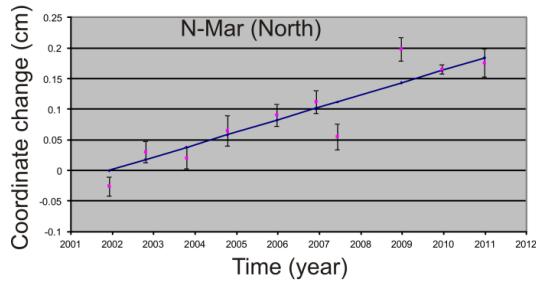
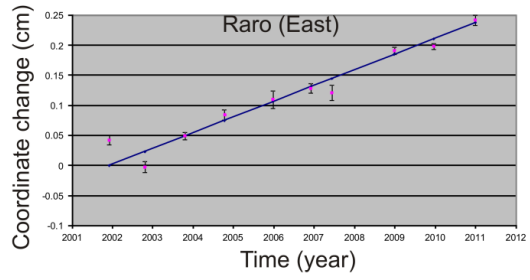
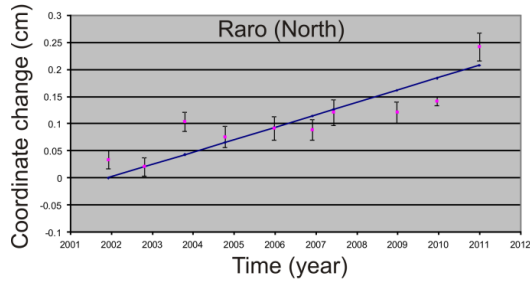
1. The seismicity is concentrated on the Kalabsha fault zone at the intersection between the E-W and N-S fault trends, particularly along its most eastern segment, which is located beneath a large area covered by water. However, the E-W Kalabsha fault system controls the seismicity in the region.
2. The seismicity can be classified into shallow and deep seismic zones. Shallow earthquakes have focal depths less than 12 km and deep events extend from 12 to 28 km.
3. The term seismic hazard is used to denote the probability of occurrence of an earthquake with the magnitude larger or equal to a particular value, within a specified region and a given time span. The combination of the previously described circumstances makes it is very difficult to estimate where the next damaging earthquake

in Aswan region may occur. The best estimate is that, it will be occurred in a place of historic activity and will be of a magnitude between 4.5 and 5.5.

4. The role of the reservoir water loading, as a supplementary source of earthquake events in the region, cannot be neglected. Therefore, it can be understood that, the earthquake activity in the area originated tectonically and the water variation works as an activation medium in triggering small earthquakes.
5. Rate of the accumulated strains is small and lies in the lowest class of the category of the strain classifications; this indicates to the stability of the region

REFERENCES

- Abdel-Monem, S. M.: 1994, Effect of water loading in inducing seismicity around aswan reservoir, Egypt. *Acta Geod. Geoph. Hung.*, 29 (1-2), 5–18.
- Abdel-Monem,, S.M.: 2005, Using compiled seismic and GPS data for hazard estimation in Egypt. *NRIAG, Journal of Geophysics*, 4, No. 1, 51–79.
- Dach, R., Hugentobler, U., Fridez, P., and Meindl, M. (eds): 2007, *Bernese GPS Software Version 5.0*, Astronomical Institute, University of Bern.
- Edel, J.E.: 1984, Statistical aspects of New England seismicity from 1975 to 1982 and implications for past and future earthquake activity. *Bull. Seism. Soc. Am.* 74, No. 4, 1311–1329.
- Epstein, B. and Lomnitz C.: 1966, A model for the occurrence of large earthquakes. *Nature*, No. 211, 954–956.
- Fuji, Y.: 1997, Estimation of continuous distribution of Earth's strain in the Kanto-Tokai district, Central Japan, with the aid of least squares collocation. *Advanced lectures on geodesy and seismology in Egypt*. August, 1996 to July, 1997. *Bull. NRIAG (Special Issue)*. 97–126.
- Gupta, H.K. and Rastogi, B.K.: 1976, *Dams and Earthquakes*. Elsevier, Amsterdam, 299 pp.
- Gupta, H.K.: 1972, *Reservoir induced seismicity*, Elsevier, Amsterdam, 364 pp.
- Gupta, H.K.: 1992, *Reservoir induced seismicity*. Elsevier, Amsterdam.
- Gutenberg, R. and Richter, C.F.: 1954, *Seismicity of the Earth and associated phenomena*. Princeton Univ. Press New Jersey, 2nd ed., 310 pp.
- Haggag, H.M., Gaber, H.H., Sayed, A.D. and Ezat, M.E.: 2008, A review of the recent seismic activity in the Southern part of Egypt (Upper Egypt). *Acta Geodyn. Geomater.*, 5, No. 1 (149), 19–29.
- Haggag, H.M. and Karrar, O.E.: 2009, The 12 – 14 April 2007 Seismic Swarm at Kalabsha area, Aswan, Egypt. *Geophys. Lett.*, 2, Faculty of Sci., Zagazig University, Egypt.
- Hassoup, A., Mahmoud, M., Gaber, H., and Elbohoty, M.: 2005, Temporal and three dimensional spatial analysis of seismicity in the lake Aswan area, Egypt. *Acta Geophysica Polonica*. 53, no. 2, 153–166.
- Howell, B.F. Jr.: 1980, A Comparison of seismic risk estimates in the Central United States. *Earthquake Notes*, No. 51, 13–19.
- Issawi, B.: 1969, *The geology of Kurkur-Dungul Area*. General Egyptian Organization for Geological



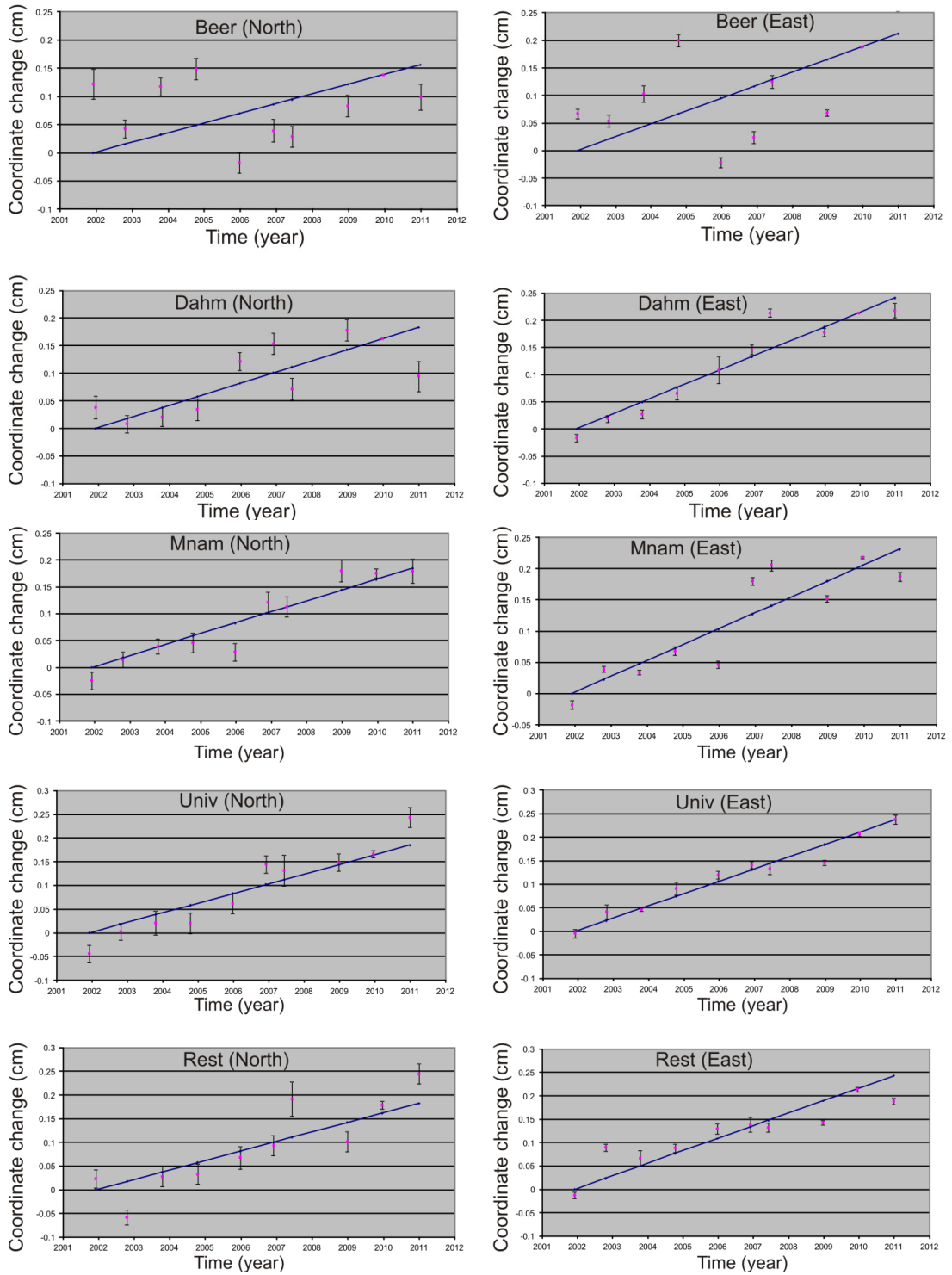


Fig. 14 Time series for Aswan network stations (these graphs represent the horizontal velocity of Aswan network), small solid circles on the plot represent an independent position estimate, typically based on three days of observations, with error bars.

- Research and Mining; Geological Survey. No. 46, 101 pp, Cairo, Egypt.
- Issawi, B.: 1978, Geology of Nubia West Area, Western Desert. Annals of the Geological Survey of Egypt. B, 237–253.
- Issawi, B.: 1982, Geology of the southwestern desert of Egypt, Annals of the Geological Survey of Egypt, 215 pp.
- Kebeasy, R.M. and Gharib A.A.: 1991, Active fault and water loading are important factors in triggering earthquake activity around Lake Aswan. *J. Geodynamics*, 14, No. 1-4, 73–83.
- Kebeasy, R.M., Maamoun, M. and Ibrahim, I.M.: 1982, Lake Aswan induced earthquake. *Bull. Internal. Inst. Seismol. Earthq. Eng.*, No. 19, 155–160.
- McClusky, S., Reilinger, S., Mahmoud, S.M., Ben Sari, D., and Tealeb, A.: 2003, GPS constraints on Africa (Nubia) and Arabia plate motions, *Geophys. J. Int.*, 155, 126–138.
- Mogi, K.: 1962b, Study of elastic shocks caused by the fracture of heterogeneous materials and its relation to earthquake phenomena. *Bull. Earthquake Res. Inst.*, 40, 125–173.
- Raafat, E., Fat-Helbary, R.E. and Haggag Mohamed, H.: 2004, Seismicity and seismotectonics of the West Kom Ombo area, Aswan, Egypt, *Acta Geodyn. Geomater.*, 1, 2 (134), 195–200.
- Rundlle, J.B.: 1989, Derivation of complete Richter magnitude frequency relation using the principle of scale in variance. *J. Geodynamics Res.*, 94, 12, 337–342.
- Scholz, C.H.: 1968, The frequency magnitude relation of micro-fracturing in rock and its relation to earthquakes. *Bull. of Seismol. Soc. Am.*, 58, 399–415.
- Simpson, D.W.: 1976, Seismicity changes associated with reservoir loading, *Eng. Geol.*, 10, 123–150.
- Simpson, D.W., Leith, W.S. and Scholz, C.H.: 1988, Two types of reservoir-induced seismicity, *Bull. Seismol. Soc. Am.*, 78, 2025–2040.
- Talwani, P.: 1997, On the nature of reservoir induced seismicity. *Pure Appl. Geophys.*, 150, 473–492.